A Hebbian approach to complex-network generation

2011 EPL 94 10002

(http://iopscience.iop.org/0295-5075/94/1/10002)

A Letters Journal Exploring the Frontiers of Physics

April 2011

EPL, **94** (2011) 10002
doi: 10.1209/0295-5075/94/10002

www.epljournal.org

A Hebbian approach to complex-network generation

E. Agliari[1,2(a)] and A. Barra[3,4]

[1] *Dipartimento di Fisica, Università degli Studi di Parma - viale Usberti 7/A, 43100 Parma, Italy, EU*
[2] *Istituto Nazionale di Fisica Nucleare, Gruppo Collegato di Parma - Parma, Italy, EU*
[3] *Dipartimento di Fisica, Sapienza Università di Roma - P.le A. Moro 5, 00182, Rome, Italy, EU*
[4] *Gruppo Nazionale di Fisica Matematica, Sezione di Roma1 - Rome, Italy, EU*

received 2 November 2010; accepted in final form 28 February 2011
published online 28 March 2011

PACS 05.50.+q – Lattice theory and statistics (Ising, Potts, etc.)
PACS 02.10.Ox – Combinatorics; graph theory
PACS 05.70.Fh – Phase transitions: general studies

Abstract – Through a redefinition of patterns in a Hopfield-like model, we introduce and develop an approach to model discrete systems made up of many, interacting components with inner degrees of freedom. Our approach highlights the intrinsic connection between the kind of interactions among components and the emergent topology describing the system itself; also, it allows to effectively address the statistical mechanics on the resulting networks. Indeed, a wide class of analytically treatable, weighted random graphs with a tunable level of correlation can be recovered and controlled. We especially focus on the case of imitative couplings among components endowed with similar patterns (*i.e.* attributes), which naturally gives rise to small-world effects. We also solve the thermodynamics (at a replica symmetric level) by extending the double stochastic stability technique: free energy, self-consistency relations and fluctuation analysis for a picture of criticality are obtained. Finally, applications are considered, with particular attention to the agreement among the non-trivial features predicted by the theory and the experimental findings.

Introduction. – The performance of most complex systems, from the cell to the Internet, emerges from the collective activity of many inner components. At an abstract level, the latter can be reduced to a series of nodes connected each other by links envisaging the interaction, *i.e.* a graph [1–3]. Such a description has led to identify classes of (topological) universality, and to evidence how experimentally revealable features, *e.g.* cliquishness, modularity or peculiar degree distribution, not only underlie a certain degree of correlation among components and/or links, but also crucially affect the behavior of the whole system [1]. This constituted a real breakthrough with respect to the previous tendency to model complex networks either as regular, homogeneous objects, such as lattices, or as purely random networks à la Erdös-Rényi (ER) [4].

In this letter we introduce and develop an approach to model collective systems where nodes are characterized by a set of attributes and pairwise interactions may, in principle, be of different nature (*e.g.* imitative, repulsive, etc.). According to the way we fix such features we can recover a broad class of weighted random graphs exhibiting tunable topological properties; this also allows to infer about the plausibility of a given modelization: the choice of a particular network must be consistent with the kind of interactions governing the system itself and vice versa.

In the second part of this work, we study the thermodynamic properties of a subset of these structures generated by a "Hebbian-like kernel"; interestingly, such an approach allows to work out the thermodynamics of a wide class of diluted graphs, even in the presence of ferromagnetic disorder on couplings.

Modelization. – Given a set of V components, we characterize each of them by a "pattern" ξ, namely a set of attributes, encoded by a binary string of length L. Then (similarly to the "hidden variable" approach [5,6]), a rule r is introduced in such a way that any couple of strings is associated to a real value which provides the pertaining coupling, $r(\xi_i, \xi_j) = J_{ij}$, ultimately generating a topology. Now, crucial for the whole approach are the way the strings are extracted and the rule r, both to be defined according to the processes one wishes to model.

For instance, for the i-th node, the μ-th entry $\xi_i^\mu = 1(\xi_i^\mu = 0)$ can represent, within a social context, the positive (negative) attitude of the i-th agent towards a

(a) E-mail: elena.agliari@fis.unipr.it

socio-political issue, or, within a biological context, the presence (absence) of a particular genetic mutation or the hydrophilic (hydrophobic) nature of a binding site in the i-th building block. In the following, in order to highlight the possible applications of our theory, we will emphasize the various features which the model is able to reproduce and we will resume them in the final discussion about possible applications.

The Hebbian-like kernel. We investigate in detail the case of biased patterns where the probability to extract any entry is $P(\xi_i^\mu = 0) = 1 - P(\xi_i^\mu = 1) = (1-a)/2$, $a \in [-1, 1]$; the rule r is given by the scalar product

$$J_{ij} = J_{ji} = \sum_{\mu=1}^{L} \xi_i^\mu \xi_j^\mu. \tag{1}$$

Notice that such a rule resembles the Hebbian one, well known in neural networks [7], apart from the shift $[-1, +1] \to [0, +1]$ in the definition of patterns; this plain replacement converts frustration into ferromagnetic dilution.

Property 1. We are therefore naturally focusing on systems where the interaction among components is stronger the larger the number of positive attributes they share.

A useful parameter to characterize a given node is the number ρ of non-null entries present in the related string: Within a mean-field approach, it can be shown that the probability for i to have degree (number of neighbors) equal to z follows a binomial distribution $P_{\rm deg}(z; a, \rho_i, V)$, where large ρ_i yields narrow (small variance) distributions peaked at large z (see fig. 1; we refer to appendix A for more details). Then, one can write the overall degree distribution as a combination of the binomials $P_{\rm deg}(z; a, \rho, V)$, each weighted on the probability $P_1(\rho; a, L)$ that a string displays ρ non-null entries:

$$\bar{P}_{\rm deg}(z; a, L, V) = \sum_{\rho=0}^{L} P_{\rm deg}(z; a, \rho, V) P_1(\rho; a, L). \tag{2}$$

This expression gives rise to a L-modal distribution where "modes", each corresponding to a different value of ρ, are solved as long as the connectivity and L are not too large in order to ensure spread distributions for z and ρ (see fig. 1, left and right panels, respectively, and [8] for more details).

Property 2. Multimodal degree distributions constitute an interesting feature of the model, as they allow to naturally discriminate between different classes of nodes possibly fulfilling different functions. In particular, nodes corresponding to a large degree are often associated to a relatively small reactivity and vice versa [9].

A more global characterization can be attained by the average link probability, considering a generic couple of nodes, neglecting any information about correlations: $p = 1 - \{1 - [(1+a)/2]^2\}^L$, so that the average degree reads as $\bar{z} = pV$. Now, for $L \to \infty$, p approaches a discontinuous

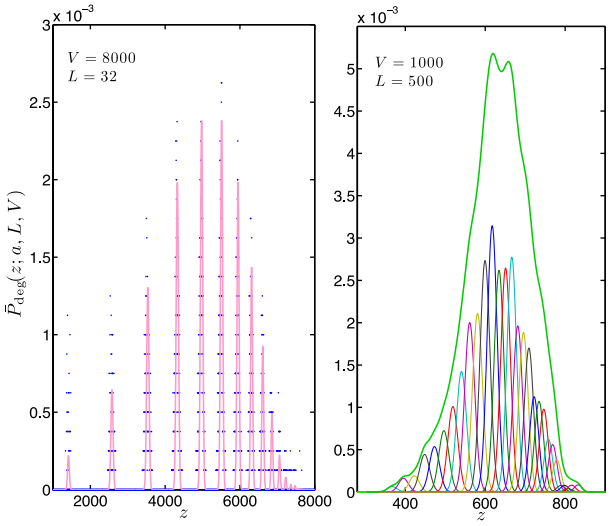

Fig. 1: (Color online) Degree distribution $\bar{P}_{\rm deg}(z;\ a,\ L,\ V)$ for systems displaying small L/V ratio and multimodal distribution (left panel) and large L/V with modes collapsing into a unimodal distribution (right panel); the chosen values of a are -0.71 and -0.92, respectively. In the former case we plot data points ($\bullet$) as well as the analytical curves consistently with eq. (2). In the latter case we show the distributions corresponding to each mode $P_{\rm deg}(z;\ a,\ \rho,\ V)$ in agreement with numerical data, as well as the overall distribution (thicker, bright curve).

function assuming value 1 when $a > -1$ and value 0 when $a = -1$. Consequently, focusing on the so-called high-storage regime (in neural networks jargon [7]) where L is linearly divergent with V, *i.e.* $L = \alpha V$, the range of values for a yielding a non-trivial topology can be characterized by means of the scaling

$$a = -1 + \frac{\gamma}{V^\theta}, \tag{3}$$

where $\theta \geqslant 0$ and γ is a finite parameter[1]. Hence, for large sizes, only values of a close to -1 are interesting (see fig. 1), while larger values of a yields $p \approx 1$ and the degree distribution is a delta function peaked at $V - 1$. Nonetheless, if one chooses L small enough such that the degree distribution gets spread, modes are still solved. Following [8], we distinguish the following regimes, holding in the thermodynamic limit (see fig. 2):

- $\theta < 1/2$, $p \to 1$, $\bar{z} \to V$ $\Rightarrow$ Fully connected (weighted) graph [10].
- $\theta = 1/2$, $p \sim 1 - e^{-\gamma^2 \alpha/4}$, $\bar{z} = O(V)$ $\Rightarrow$ Linearly diverging connectivity. Within a MF description the (weighted) ER graph with finite link probability is recovered [11].
- $1/2 < \theta < 1$, $p \sim \gamma^2 \alpha V^{1-2\theta}/4$, $\bar{z} = O(V^{2-2\theta})$ $\Rightarrow$ Extreme dilution regime: $\lim_{V\to\infty} \bar{z}^{-1} = \lim_{V\to\infty} \bar{z}/V = 0$ [12].

[1] Since $a \in [-1, 1]$, we have that $0 \leqslant \gamma \leqslant 2\, V^\theta$; in particular, when $\theta = 0$ the upper bound for γ is 2.

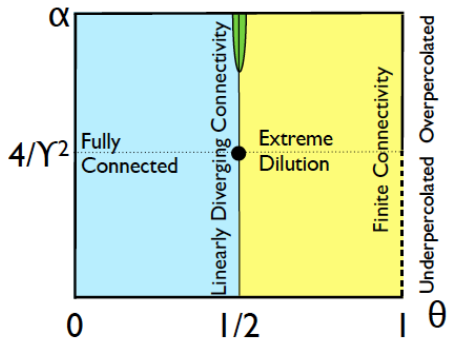

Fig. 2: (Color online) Phase diagram representing the topology of the graph as the parameters θ and α are varied; notice that the scale for α is specified in terms of γ^2. In the region on the left (blue) disorder on couplings is present, while on the right side (yellow) this disorder is lost but topological inhomogeneity is still present. In the narrow central region (green) both kinds of disorder may coexist.

– $\theta = 1$, $p \sim \frac{\gamma^2\alpha}{4V}$, $\bar{z} = O(V^0) \Rightarrow$ Finite connectivity regime [13]. Within a MF description $\gamma^2\alpha/4 = 1$ corresponds to a percolation threshold.

Larger values of θ determine a disconnected graph with vanishing average degree. Therefore, θ coarsely controls the connectivity regime of the network, while γ and α (which turn out to be intrinsically related) allow a fine tuning.

Up to now we just focused on topological disorder; as for couplings, we can still detect "modes", each characterized by J_ρ representing the average strength for links stemming from a node associated to a string with ρ non-null entries. While J_ρ provides a measure of the local "field" seen by a single node, a global description can be attained by the overall average coupling $\bar{J} \equiv \sum_\rho J_\rho P_1(\rho; a, L)$, taken over the whole graph; the two quantities are related via $J_\rho = \sqrt{\bar{J}}\rho/L$ [8]. As we will see in the next section, despite the self-consistence relation (more sensible to local conditions) is influenced by $\sqrt{\bar{J}}$, the critical behavior occurs at $\beta_c = \bar{J}^{-1}$, consistently with a manifestation of a collective, global effect.

By looking in more detail at the coupling distribution holding in the thermodynamic limit and for values of a determined by eq. (3), we find that, for $1/2 < \theta \leqslant 1$, nodes are pairwise either non-connected or connected due to one single matching among the relevant strings. For $\theta = 1/2$ this still holds when $\alpha\gamma^2/4 \ll 1$, which corresponds to a relatively high-dilution regime, otherwise some degree of disorder is maintained. On the other hand, for $\theta < 1/2$, while topological disorder is lost, disorder on couplings is still present. However, for $\theta = 0$ and $\gamma = 2$, the coupling distribution gets peaked at $J = L$ and, again, disorder on couplings is lost [8].

Small-world properties. Among the properties defining "small-world" networks [14] there is a high degree of transitivity, that is neighborhood cohesiveness, which is usually quantified by the (average local) clustering coefficient c to be possibly compared with the one expected for a comparable (*i.e.* displaying the same average degree) ER graph, namely $c^{\mathrm{ER}} = \bar{z}/V$ [1].

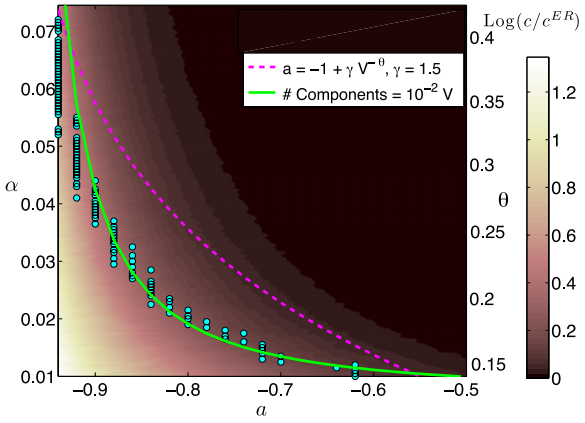

Fig. 3: (Color online) Natural logarithm of c/c^{ER} as a function of α and a for a system with $V = 2000$. When a follows the scaling of eq. (3) with $\gamma = 1.5$ (dashed line) the ratio is $\approx$4, meaning high clustering. Data points (•), fitted by a power law $\sim(1+a)^\eta, \eta \approx 1.5$, demarcate the region where the graph is made of 20 components (the giant one plus isolated nodes).

Property 3. For the graph generated by eq. (1), the neighborhood V_i of i is made up of all nodes displaying at least one non-null entry corresponding to any non-null entries of ξ_i. This condition biases the distribution of strings relevant to nodes $\in V_i$, so that they are more likely to be connected with each other. This is also confirmed numerically: fig. 3 shows that $c/c^{\mathrm{ER}} > 1$ in a wide region of the plane (α, a), especially in the region of high dilution.

Property 4. This kind of link correlation allows to detect communities densely and strongly linked up, so that the role of weak ties is crucial in maintaining the graph connected, while strong ties turn out to be redundant [15,16].

Thermodynamics. – When dealing with the thermodynamical properties of these networks, we first paste V variables (spins) $\sigma = \{-1, +1\}$ on the nodes and define the Hamiltonian

$$H(\sigma; \xi) = \frac{-1}{2\alpha V^{2(1-\theta)}} \sum_{i<j}^{V} \sum_{\mu}^{L} \xi_i^\mu \xi_j^\mu \sigma_i \sigma_j, \qquad (4)$$

formally identical to a Hopfield model, apart from the normalization which accounts for quenched variables non-symmetrical with respect to zero. From eq. (4) the standard package of disordered statistical mechanics can be introduced: the partition function $Z_V(\beta; \xi) = \sum_\sigma \exp[-\beta H_V(\sigma; \xi)]$, the Boltzmann state $\omega(.) = \sum_\sigma .e^{-\beta H_V(\sigma;\xi)}/Z_V(\beta; \xi)$, and the related free energy $A(\beta, \gamma, \theta) = \lim_{V\to\infty} V^{-1}\mathbb{E} \log Z_V(\beta; \xi)$, where $\mathbb{E}$ averages over the quenched distributions of the bit strings ξ. At first, in order to obtain an explicit expression of the

free energy, through the Hubbard-Stratonovick transform we map the partition function of our model into a bipartite ER one, whose parties are the V Ising spins and L auxiliary Gaussian fields z as

$$Z_V(\beta;\xi) = \sum_{\sigma} \int_{-\infty}^{+\infty} \prod_{\mu=1}^{L} \mathrm{d}\mu(z_\mu) e^{\frac{\sqrt{\beta/\alpha}}{V^{1-\theta}} \sum_{i,\mu}^{V,L} \xi_{i,\mu}\sigma_i z_\mu}, \quad (5)$$

namely a system ruled by the following "effective Hamiltonian" $\tilde{H} = (1/\sqrt{\beta\alpha}V^{1-\theta}) \sum_{i,\mu}^{V,L} \xi_{i\mu}\sigma_i z_\mu$: Two parties interacting with Bernouillian dilution and constant weights. As shown in appendix B, for these systems it is possible to extend the double stochastic stability technique recently developed in [17]; as a consequence, once introduced the proper order parameters of the theory, we can directly focus on the resulting thermodynamical properties.

To figure out our order parameters, as replica symmetry (RS) is expected to be conserved in ferromagnetic diluted networks, we naturally avoid (multi)-overlaps by defining

$$M_{l_b} = \frac{1}{V} \sum_i \omega_{l_b+1}(\sigma_i), \quad N_{l_c} = \frac{1}{L} \sum_{\mu}^{L} \omega_{l_c+1}(z_\mu),$$

where the index in ω means that we are considering all the possible magnetizations built trough only l_b+1 links inside the graph (as the graph is no longer weighted, it is a microcanonical decomposition of the observable in subclusters conceptually close to the one introduced in [18]). The averaged order parameters $\langle M\rangle = \sum_{l_b} P(l_b) M_{l_b}$, and $\langle N\rangle = \sum_{l_c} P(l_c) N_{l_c}$, can then be obtained being $P(l)$ the probability that l links are present, namely

$$P(l_b) = \binom{V}{l_b} \left(\frac{1+a}{2}\right)^{V-l_b} \left(\frac{1-a}{2}\right)^{l_b}, \quad (6)$$

$$P(l_c) = \binom{L}{l_c} \left(\frac{1+a}{2}\right)^{L-l_c} \left(\frac{1-a}{2}\right)^{l_c}. \quad (7)$$

We can now explicitly write down the free energy as

$$A(\beta,\gamma,\theta) = \log 2 + \lim_{V\to\infty} \frac{\gamma}{2V^\theta} \langle \log\cosh(\sqrt{\beta}\bar{N}V^\theta)\rangle + \frac{\beta\gamma^2}{8}\langle\bar{M}\rangle^2 - \frac{\sqrt{\beta}\gamma}{2}\langle\bar{M}\rangle\langle\bar{N}\rangle,$$

where the bars denote the "replica symmetric" (*i.e.* delta-distributed over their means) values (see appendix B).

Further, by extremizing the free energy with respect to the order parameters [17] we get the self-consistent relation $\langle\bar{N}\rangle = \langle\bar{M}\rangle\sqrt{\beta}\gamma/2$, which allows to express the whole theory only via $\langle\bar{M}\rangle$ (as expected looking at the original Hamiltonian (4)). Consequently, we can explicitly develop the various cases of interest, in particular:

– $\theta = 0$: Fully connected, weighted regime.

This case recovers the Curie-Weiss (CW) model and, specifically, the upper bound of γ (*i.e.* $\gamma = 2$) gives the unweighted fully connected structure. Consistently, its free energy and related self-consistency turn out to be

$$A(\beta,\ \gamma\ =\ 2,\ \theta = 0) = \log 2 + \frac{\gamma}{2}\log\cosh\left(\frac{\beta\gamma}{2}\bar{M}\right) - \frac{\beta\gamma^2}{8}\bar{M}^2, \quad \bar{M} = \tanh\left(\frac{\beta\gamma}{2}\bar{M}\right). \quad (8)$$

Note that, as there is only one possible network built with all links, all the subgraph magnetizations collapse into only one, namely $P(\bar{M}) = \delta(\bar{M} - M_{CW})$, where M_{CW} is the standard CW magnetization. Furthermore, note that for $\gamma = 2$ we recover exactly the CW thermodynamics.

– $\theta = 1/2$: Standard dilution and ER regime.

With a scheme perfectly analogous to the previous one we can write down the free energy and its related self-consistent equation as

$$A(\beta,\ \gamma,\ \theta\ =\ 1/2) = \log 2 + \lim_{V\to\infty}\left[\frac{\gamma}{2\sqrt{V}} \cdot \log\cosh\left(\frac{\beta\gamma}{2}\sqrt{V}\langle\bar{M}\rangle\right) - \frac{\beta\gamma^2}{8}\langle\bar{M}\rangle^2\right], \quad (9)$$

$$\langle\bar{M}\rangle = \lim_{V\to\infty} \tanh\left(\frac{\beta\gamma}{2}\sqrt{V}\langle\bar{M}\rangle\right). \quad (10)$$

Fictitious diverging contributions emerge in the thermodynamic limit because the normalization we chose for the Hamiltonian (4) gives the correct extensivity for the fully connected case only, while for the ER regime we expect a normalization factor $O(V^{-1})$. Note in fact that the argument of the logarithm of the hyperbolic cosine can be read as $\beta\sqrt{\bar{J}}V\langle\bar{M}\rangle$. As in standard approaches [11], it is enough to renormalize the coupling by scaling it with the amount of nearest neighbors [19] (which in the ER dilution grows linearly with the volume size).

For intermediate values of θ, as well as for $\theta > 1/2$ (corresponding to an extreme dilution regime), it is possible to apply a scheme analogous to the previous ones and to write down straightforwardly an expression for the related free-energy and the coupled self-consistencies.

Property 5. In general, we find that the effective field felt by a generic spin does not scale linearly with the average coupling strength $\bar{J}$ as one would expect naively, but, rather, it scales as the square root of $\bar{J}$; of course this effect disappears approaching the CW limit where $\sqrt{\bar{J}} \to \bar{J} \to 1$. Moreover, since the interaction matrix in the Hamiltonian has been normalized (*i.e.* is bounded by one), $\sqrt{\bar{J}} > \bar{J}$.

However, this feature, which is a consequence of the diverging variance in the bitstring distribution [8], does not affect the transition line that scales consistently with a manifestation of a collective, global effect, as $\beta_c \propto \bar{J}^{-1}$ (the proof is reported in appendix C).

Discussion. – In this work we formalized the generation of collective systems made up of nodes characterized by a set of attributes and in mutual interaction, highlighting how the definition of attributes and of the way the components interact impose a specific topology on the emerging network, with important consequences on the overall system performance.

In particular, we focused on imitative (*i.e* positive coupling) systems where the interaction strength J_{ij} among two nodes i and j is larger the more similar the related attributes, and we showed that a wide class of topologies can be recovered, exhibiting small-world features and multi-modal degree distributions.

The thermodynamics of these systems has also been addressed showing that for such disordered, diluted ferromagnets a second-order phase transition occurs at a critical temperature T_c corresponding to the average coupling strength $\bar{J}$. On the other hand, by looking at the self-consistent relations (being more sensible to local conditions), we showed that the field felt by the generic spin scales like $\sqrt{\bar{J}}$ (which indeed corresponds to the average local field) instead of $\bar{J}$ as expected from classical ferromagnetic theory: this accounts for a superlinear contribution in the exchanges among the elements ascribable to the high cliquishness of the underlying network.

Now, due to the generality of the approach, one can introduce slight variations with respect to the model analyzed here, possibly yielding dramatic changes in the global layout of the graph (*e.g.* scale-free degree and/or coupling distributions) and properly extend the thermodynamic analysis. Indeed, the framework developed here may open a new alternative (*e.g.* to replica trick) for trying to solve spin glasses on correlated networks (by considering rules r not positive defined), whose mathematical difficulty is still prohibitive.

Finally, we briefly discuss two paradigmatic examples of our theory, concerning social [20] and immunological [21,22] networks.

In social networks agents are represented by nodes and links among them denote a kind of relationship. As pointed out by Brock and Durlauf [23], the interactions among agents are essentially imitative and the larger the number of interests they share, the stronger their interaction (*Property 1*). Interestingly, within our model this prescription is sufficient to give rise to another pivotal point, namely small-world features (*Property 3*), in agreement with Milgram's experiment [24] (showing that the average distance among nodes is relatively short) and with Watts and Strogatz's model [14] (exhibiting high degree of transitivity). Moreover, the weight distribution determined by eq. (1) also recovers Granovetter's seminal observation [20] about the crucial role of weak ties in keeping the network connected (*Property 4*).

As for theoretical immunology, we recall Jerne's [25] original formulation of the idiotypic network, whose nodes are lymphocytes and their interaction stems from the complementarity among the related set of epitopes; this can be captured by a rule r which privileges complementary entries [21,22], still retaining the hierarchy yielding a multimodal degree distribution. This aspect nicely matches with the fundamental contribution due to Varela [26], who showed the existence of connectivity classes such that the more connected lymphocytes and the more lazy to respond to external antigens (*Property 2*). Moreover, the immune network displays intrinsic correlations which may give rise to non-trivial collective behaviors (*Property 5*), ultimately affecting the immune response.

* * *

This work is supported by FIRB grant RBFR08EKEV.

Appendix A. – Given a string ξ_i of length L, with entries independently extracted according to $P(\xi_i^\mu = 0) = 1 - P(\xi_i^\mu = 1) = (1-a)/2$, $a \in [-1,1]$, we define $\rho_i \equiv \sum_{\mu=1}^{L} \xi_i^\mu$. Due to the independence underlying the extraction of each entry, ρ follows a binomial distribution

$$P_1(\rho; a, L) = \binom{L}{\rho} \left[\frac{(1+a)}{2}\right]^{\rho} \left[\frac{(1-a)}{2}\right]^{L-\rho} \equiv \mathcal{B}(\rho; L, (1+a)/2), \tag{A.1}$$

with average $\bar{\rho}_{a,L} = L(1+a)/2$. Moreover, it can be shown that the probability for two string ξ_i and ξ_j, displaying respectively ρ_i and ρ_j non-null entries, to be connected is

$$P_{\text{link}}(\rho_i, \rho_j; L) = 1 - \frac{(L-\rho_i)!(L-\rho_j)!}{[L!(L-\rho_i-\rho_j)!]}. \tag{A.2}$$

By averaging over, say ρ_j, one finds the expected link probability $P_{\text{link}}(\rho_i, a) = 1 - [(1-a)/2]^{\rho_i}$ for the node i. Then, the probability that i has degree (number of neighbors) equal to z follows as the binomial $P_{\text{deg}}(z; a, \rho_i, V) = \mathcal{B}(z; V, P_{\text{link}}(\rho_i, a))$. Due to the average over ρ_j, this corresponds to a MF approach where we treat all the remaining nodes in the average; this works finely for V large and ρ_i not too small (see fig. 1).

As for the whole system, the global degree distribution can be written as the average of $P_{\text{deg}}(z; a, \rho_i, V)$ over $\rho \in [0, L]$, where each term is weighted by $P_1(\rho; a, L)$, as shown in eq. (2).

Finally, we notice that the average link probability p for two generic nodes can be estimated from eq. (A.1) and eq. (A.2) as

$$\begin{aligned} p &= \sum_{\rho_i=0}^{L} \sum_{\rho_j=0}^{L} P_1(\rho_i; a, L) P_1(\rho_j; a, L) P_{\text{link}}(\rho_i, \rho_j; L) \\ &= 1 - \left[1 - \left(\frac{1+a}{2}\right)\right]^{L}. \end{aligned} \tag{A.3}$$

Appendix B. – Dealing with the free energy built by the partition function (see eq. (5)) we enlarge the

technique of the double stochastic stability [17] by introducing the following interpolating structure:

$$A(t) = \frac{\mathbb{E}}{V}\log\sum_{\sigma}\int_{-\infty}^{+\infty}\prod_{\mu}^{L}\mathrm{d}\mu(z_\mu)\exp\Bigg[t\frac{\sqrt{\beta/\alpha}}{V^{1-\theta}} \times\sum_{i,\mu}\xi_{i\mu}\sigma_i z_\mu+(1-t)\left(\sum_{l_c=1}^{L}b_{l_c}\sum_{i}^{V}\eta_i\sigma_i + \sum_{l_b=1}^{V}c_{l_b}\sum_{\mu}^{L}\chi_\mu z_\mu\right)\Bigg], \tag{B.1}$$

where now $\mathbb{E}=\mathbb{E}_\xi\mathbb{E}_\eta\mathbb{E}_\chi$, b_{l_c} [with $l_c\in(1,\dots,L)$], and c_{l_b} [with $l_b\in(1,\dots,V)$] are real numbers (possibly functions of β, γ, θ) to be set *a posteriori*.

Note that $A(t=1)$ is our goal, while $A(t=0)$ is straightforward as it involves only one-body calculations. So we want to use the fundamental theorem of calculus to get a sum rule, as

$$A(1)=A(0)+\int_0^1[\partial A(t')/\partial t']_{t'=t}\,\mathrm{d}t,$$

which ultimately implies the evaluation of the t-streaming of eq. (B.1) and the explicit calculation of $A(0)$.

By a long but straightforward calculation, and using a bar to denote the replica symmetric order parameters (namely $\bar{M},\bar{N}$), we find that $\partial_t A(t)=S(t)-\sqrt{\beta}\gamma/2\sum_{l_b}\sum_{l_c}P(l_b)P(l_c)\bar{M}_{l_b}\bar{N}_{l_c}$, where the fluctuation source $S(t)$ is proportional to $\langle(M-\bar{M})(N-\bar{N})\rangle$ and can be neglected at the RS level.

The replica symmetric solution $A_{RS}(t=1)$ can then be written as $A_{RS}(t=1)=A(t=0)-\sqrt{\beta}\gamma\langle M\rangle\langle N\rangle/2$, whose explicit expression is reported in eq. (8).

Appendix C. – In order to prove that $\beta_c=\bar{J}^{-1}$, we analyze the fluctuations of the rescaled order parameters $\langle\mathcal{M}\rangle=\sqrt{V}\langle M-\bar{M}\rangle$, $\langle\mathcal{N}\rangle=\sqrt{L}\langle N-\bar{N}\rangle$ checking where they diverge, this defines the onset of criticality: At first we need to derive the t-streaming of the squares of these objects (*i.e.* $\langle\mathcal{M}^2\rangle,\langle\mathcal{M}\mathcal{N}\rangle,\langle\mathcal{N}^2\rangle$), which lead to a system of coupled ordinary differential equations in t, namely

$$\langle\dot{\mathcal{M}}^2\rangle=2\langle\mathcal{M}^2\rangle\langle\mathcal{M}\mathcal{N}\rangle, \tag{C.1}$$

$$\langle\dot{\mathcal{M}\mathcal{N}}\rangle=\langle\mathcal{M}^2\rangle\langle\mathcal{N}^2\rangle+\langle(\mathcal{M}\mathcal{N})^2\rangle, \tag{C.2}$$

$$\langle\dot{\mathcal{N}^2}\rangle=2\langle\mathcal{N}^2\rangle\langle\mathcal{M}\mathcal{N}\rangle. \tag{C.3}$$

Then we have to start the "motion" at $t=0$ (this Cauchy condition is straightforward to be evaluated as, in $t=0$, everything is factorized) and propagate it trough $t=1$; the obtained fluctuations will be meromorphic functions, whose pole defines the critical point [18].

By using Wick theorem to express four-point correlations through series of two-point correlations [27] and due to internal symmetries reflecting the MF interactions among the two parties [8], the plan is fully solvable and all these fluctuations, as well as the correlation $\langle\mathcal{M}\mathcal{N}\rangle$, are found to diverge on the same $\beta_c=\bar{J}^{-1}$, as intuitively expected.

REFERENCES

[1] Albert R. and Barabási A.-L., *Rev. Mod. Phys.*, **74** (2002) 47; Dorogovtesev S. N. and Mendes J. F. F., *Adv. Phys.*, **51** (2002) 1079; Newman M. E. J., *SIAM Rev.*, **45** (2003) 167.

[2] Gallagher Richard and Appenzeller Tim, *Science*, **284** (1999) 79.

[3] Rozenfeld H. D., *Structure and Properties of Complex Networks: Models Dynamics Applications* (VDM Verlag) 2008.

[4] Erdös P. and Rényi A., *Publ. Math. Debrecen*, **6** (1959) 290297.

[5] Caldarelli G., Capocci A., De Los Rios P. and Muñoz M. A., *Phys. Rev. Lett.*, **89** (2002) 258702.

[6] Boguñá M. and Pastor-Satorras R., *Phys. Rev. E*, **68** (2003) 036112.

[7] Amit D. J., *Modeling Brain Functions. The World of Attractor Neural Networks* (Cambridge Press) 1988.

[8] Barra A. and Agliari E., *J. Stat. Mech.* (2011) P02027.

[9] Palla G., Lovász L. and Vicsek T., *Proc. Natl. Acad. Sci. U.S.A.*, **107** (2010) 7640.

[10] Barra A., *J. Stat. Phys.*, **132** (2008) 787.

[11] Agliari E., Barra A. and Camboni F., *J. Stat. Mech.* (2008) P10003.

[12] Watkin T. L. H. and Sherrington D., *Europhys. Lett.*, **14** (1991) 791.

[13] Hatchett J. P. L., Perez-Castillo I., Coolen A. C. C. and Skantzos N. S., *Phys. Rev. Lett.*, **95** (2005) 117204.

[14] Watts D. J. and Strogatz S. H., *Nature*, **393** (1998) .

[15] Agliari E. and Barra A., *A statistical mechanics approach to Granovetter theory*, available at arXiv:1012.1272.

[16] Agliari E., Cioli C. and Guadagnini E., *Percolation on correlated random networks*, submitted.

[17] Barra A., Genovese G. and Guerra F., *J. Stat. Phys.*, **140** (2010) 4.

[18] Barra A. and Guerra F., *J. Math. Phys.*, **49** (2008) 125217.

[19] De Sanctis L. and Guerra F., *J. Stat. Phys.*, **132** (2008) 759.

[20] Granovetter M. S., *Sociol. Theory*, **1** (1983) 201.

[21] Barra A. and Agliari E., *J. Stat. Mech.* (2010) P07004.

[22] Barra A. and Agliari E., *Physica A*, **389** (2010) 5903.

[23] Brock W. and Durlauf S., *Rev. Econ. Stud.*, **68** (2001) 235.

[24] Milgram S., *Psychol. Today*, **2** (1967) 60.

[25] Jerne N. K., *Ann. Immunol.*, **125** (1974) 382.

[26] Stewart J., Varela F. J. and Coutinho A., *J. Autoimmun.*, **2** (1989) 862.

[27] Mandl F. and Shaw G. G., *Quantum Field Theory* (John Wiley and Sons) 1993.